Theoretical Investigation of the Ground-State Properties of DMTTF−CA: A Step toward the Understanding of Charge Transfer Complexes Undergoing the Neutral-to-Ionic Phase Transition

Vincent Oison*

L2MP UMR6137 CNRS, case 151, Faculté Saint-Jérôme, 13397 Marseille Cedex 20, France

Philippe Rabiller†

GMCM, UMR6626 CNRS, Université Rennes 1, Campus de Beaulieu, Bât 11A, 35042 Rennes Cedex, France

Claudine Katan‡

SESO, UMR6510 CNRS, Université Rennes 1, Campus de Beaulieu, Bât 10A, 35042 Rennes Cedex, France

Received: June 18, 2004; In Final Form: September 13, 2004

A detailed theoretical study based on first-principles DFT calculations is reported for the charge transfer complex 2,6-dimethyltetrathiafulvalene-*p*-chloranil (DMTTF−CA). Charge transfer estimates reveal that no periodic ordering of neutral and ionic layers is obtained in the low-temperature phase of DMTTF−CA. Similarities and differences with other mixed-stack charge transfer complexes are discussed with the help of a topological analysis of the electron density. Our results also show that the most popular model in this field, which is based on the balance between the cost of ionization and the gain in Madelung energy, should be used with great care. These molecules are far from being point charges, and molecular deformation and polarization should not be ignored.

1. Introduction

Mixed-stack organic charge transfer compounds appear as promising candidates for the fundamental study of nonlinear excitations and cooperativity in molecular materials.[1,2] These quasi-one-dimensional systems are made of mixed stacks with alternating donor (D) and acceptor (A) molecules. They have been extensively studied over the last 20 years for their original neutral−ionic phase transitions (NITs)[3,4] observed under temperature and/or pressure. Very recently, this class of materials has gained renewed interest after the experimental demonstration that the neutral (N) state can be induced by photoirradiation of the ionic (I) state or vice versa[5] and the possibility of performing a time-resolved crystallographic study of such a transformation at the picosecond time scale.[1]

The TTF−CA complex made from tetrathiafulvalene (D = TTF) and *p*-chloranil (A = CA) molecules is considered as the prototype compound for NIT.[4] At atmospheric pressure, it undergoes a first-order (symmetry-breaking) NIT at a critical temperature of about 80 K leading to a ferroelectric low-temperature phase. According to vibrational spectroscopy[6] and charge transfer absorption spectra,[7] the charge transfer (ρ) has been estimated to be about 0.2 e^- in the neutral high-temperature phase and 0.7 e^- in the ionic low-temperature phase.

The DMTTF−CA[2,8−12] complex differs from TTF−CA by replacing two hydrogens of the TTF molecule by two methyl groups in the trans position. At room temperature, it presents a continuous or weak first-order transition at a critical temperature of about 65 K, which leads to the loss of inversion symmetry. The initially planar D and A are both deformed and displaced to form a DA pair along the stacking axis similarly to what has been observed in TTF−CA.[8,13] Interestingly, the phase transition is accompanied by a doubling of the unit cell, resulting in two different type of planes. From IR spectra obtained on powder samples, Aoki and co-workers[10] concluded the coexistence of N and I species. Relating these two observations, Collet and co-workers[8] inferred that DMTTF−CA presents at low temperature a periodic ordering of neutral and ionic planes. This has been related to the staging effect proposed by Hubbard and Torrance.[14] It is claimed that the homogeneous ionization of the crystal is not favored because of repulsive interactions between adjacent stacks. It is important to notice that in this simple picture the large spatial extension of the molecules when comparing to intermolecular distances as well as the molecular tilt are completely disregarded. Recent experimental studies on single crystals using polarized light did not confirm the coexistence of N and I species in the low-temperature (LT) phase of DMTTF−CA.[11,12]

Numerous theoretical approaches have been applied for the understanding of the mechanism of NITs and the photoconversion observed in these charge transfer crystals. Despite its simplicity, the balance between the energy needed to ionize molecules and the gain in the Madelung energy, introduced by Torrance and co-workers[4] more then twenty years ago, is still often put forward.[1,8,11,15] However, it is clear that in these systems, unlike in other classes of compounds, no dominant interaction has been evidenced, and the nature of NIT must be related to a subtle interplay of different types of interactions.

* voison@L2MP.fr; former address: GMCM, UMR6626 CNRS − Université Rennes 1, Campus de Beaulieu Bât. 11A, 35042 Rennes Cedex, France

† philippe.rabiller@univ-rennes1.fr

‡ claudine.katan@univ-rennes1.fr; former address: GMCM, UMR6626 CNRS − Université Rennes 1, Campus de Beaulieu Bât. 11A, 35042 Rennes Cedex, France

10.1021/jp047353v CCC: $27.50
Published on Web 11/16/2004

The main purpose of this work is to reconsider the relevance of such a simple picture and the possible ordering of N and I layers in DMTTF−CA. Starting from first-principles density functional theory (DFT) calculations, we present here a thorough study of this D−A crystal, in the same spirit as in our previous work on TTF−CA.[16] In Section 2, we present briefly the computational details of our theoretical study. In Section 3, we summarize the main results concerning the experimental structure and discuss the experimental determinations of the charge transfer. The different contributions to the total energy of the crystal are then presented in Section 4 where the intramolecular energy is deduced from ab initio calculations performed for isolated neutral and charged molecules, and intermolecular interactions are described by classical pair potentials. The deduced equilibrium charge transfer for both phases is analyzed and compared with experimental data. Section 5 is devoted to ab initio calculations in the crystal. We present a brief analysis of valence bands (VB) and conduction bands (CB) using a tight binding model fitted to ab initio results. The total 3D electron density is then analyzed using Bader's topological approach.[17] This offers a quantitative way of analyzing the main intermolecular interactions. The last section is devoted to discussion and comparison to other D−A crystals.

2. Computational Details

We performed electronic structure calculations within the framework of DFT using the local density approximation (LDA) parametrization by Perdew and Zunger,[18] Becke's gradient correction to the exchange energy,[19] and Perdew's gradient correction to the correlation energy.[20] The main difficulty in treating the molecular compounds of this family is the presence of a nonnegligible contribution of dynamical electronic interactions of the van der Waals type. They are known to be poorly described within traditional DFT approximations, more advanced treatments being far too time-consuming for such complex systems. Nevertheless, we believe that a significant charge transfer between D and A makes our ab initio results reliable for the determination of the occupied electronic states, especially in the LT phase where electrostatic interactions are large. We used the projector-augmented wave (PAW) method,[21] which uses augmented plane waves to describe the full wave functions and densities without shape approximation. The core electrons are described within the frozen core approximation. The band structure calculations have been carried out with a plane wave cutoff of 30 Ry for the wave function and 120 Ry for the densities.

Ab initio calculations on isolated molecules were carried out using supercells, with the molecules being electrostatically decoupled from their periodic images according to the technique described in ref 22. Atomic point charges are deduced from this technique. We verified that each supercell is large enough to ensure a negligible overlap between periodic images.

Ab initio calculations in crystals were performed using experimental data deduced from X-ray scattering at 40 K (LT phase) and 300 K (high-temperature, HT, phase).[8] Because of the very large uncertainty regarding the value of C−H bond lengths, all have been fixed at 1.08 Å. The version of the Car−Parrinello (CP)-PAW code used considers only **k**-points where the wave functions are real. (Note: More recent versions of the CP-PAW code work with all kinds of **k**-points.) To increase the number of **k**-points along **a***, we had to double and triple the unit cell along the **a** direction. As for TTF-2,-5Cl_2BQ[23] and TTF−CA,[16] results are well-converged with three **k**-points: Γ(0,0,0), X/2(1/2,0,0), and X(1,0,0), along **a***.

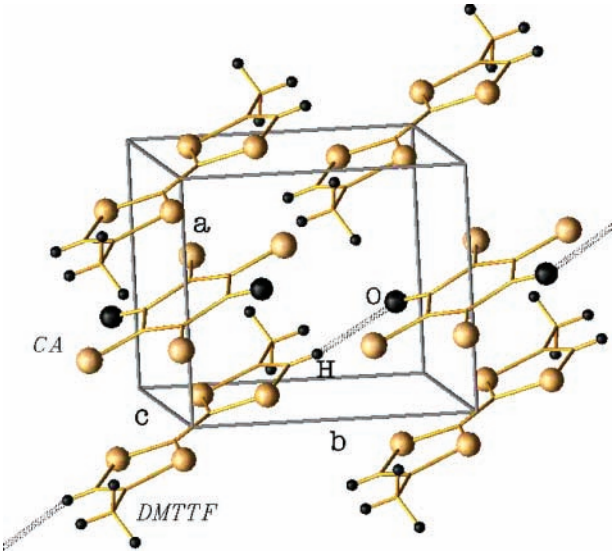

Figure 1. Representation of the high-temperature crystalline structure of DMTTF−CA; for clarity, only few molecules are shown.

The topological analysis was performed using the new *InteGriTy* software package[24] which achieves topological analysis following Bader's approach[17] on electron densities given on 3D grids; a grid spacing close to 0.1 au has been chosen. As it requires very accurate electron densities, we increased the plane wave cutoff for the wave functions to 50 Ry.

3. Experimental Structure and Charge Transfer Determination

3.1. Experimental Structure. The DMTTF−CA LT and HT structures are deduced from X-ray scattering at 40 and 300 K, respectively.[8,10] The HT crystalline structure is represented in Figure 1. At 300 K, the space group is $P\bar{1}$ with $a = 7.269$ Å, $b = 7.673$ Å, $c = 8.514$ Å, $\alpha = 95.87°$, $\beta = 103.91°$, and $\gamma = 91.87°$. There is one chain per unit cell with an alternation of DMTTF and CA molecules along the stacking axis *a* when using the conventional triclinic unit cell.[8] At 40 K, the symmetry is triclinic, and the space group is *P*1 with $a = 7.099$ Å, $b = 7.563$ Å, $c = 16.937$ Å, $\alpha = 95.77°$, $\beta = 104.21°$, and $\gamma = 91.02°$. The unit cell is doubled along the *c* direction leading to an alternation of two symmetrically different types of planes perpendicular to the *c* axis. Because of the loss of inversion symmetry, DMTTF and CA are slightly distorted and displaced and form DA pairs in the *a* direction. This distortion is quite similar to the one observed in TTF−CA. Inside a given plane, the arrangement is ferroelectric, whereas it is antiferroelectric along the *c* direction. We denote hereafter "pl1" the planes where the experimental central C═C bond length of DMTTF−CA is 1.367 Å and "pl2" the planes where this distance is 1.379 Å.[8]

3.2. Discussion on the Experimental Determination of Charge Transfer. Experimentally, the charge transfer ρ inside D−A complexes was determined indirectly by using structural[8,9,13,25] or spectroscopic measurements: reflectivity spectra on single crystals,[7,11,12] IR absorption on powder samples,[10,26] or Raman scattering on needles.[27] In DMTTF−CA, the first estimation of ρ was done by Aoki and co-workers[10] from IR absorption on powder. Their estimation is based on the frequency variation of the b_{1u} mode corresponding to the C═O stretching mode. In agreement with the estimation deduced from polarized IR reflection spectra on a single crystal,[11,12] they found a value of ρ of 0.2 e^- in the HT phase. In contrast, the value of

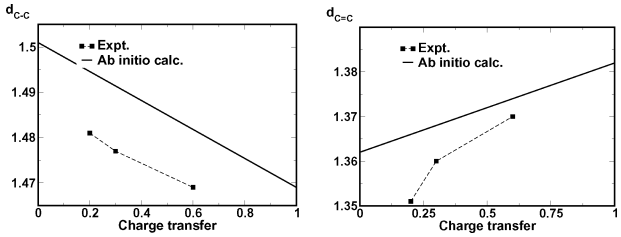

Figure 2. Variation of the inner C═C (right) and C−C (left) bond lengths of CA in angstroms as a function of the charge transfer ρ. Experimental values and ρ taken from ref 8 (squares), and calculated values obtained by geometry optimization of charged molecules (solid line).

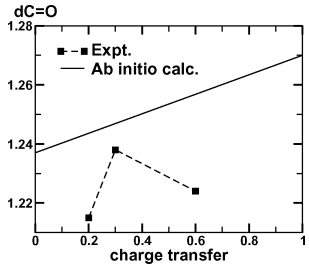

Figure 3. Variation of the C═O bond length of CA in angstroms as a function of the charge transfer ρ. Experimental values and ρ taken from ref 8 (squares), and calculated values obtained by geometry optimization of charged molecules (solid line).

ρ in the LT phase is controversial. Because of the existence of two peaks near the C═O frequency from IR absorption spectra on powder samples at low temperature, Aoki and co-workers[10] concluded the coexistence of two species of DA pairs called neutral and ionic and having, respectively, an ionicity of 0.3 and 0.6 e^-. As pointed out by Horiuchi and co-workers,[11] the possible presence of an a_g mode around 1600 cm^{-1} [28] has been disregarded. (Note: Mode splitting due to the lack of symmetry of the molecules has also been ignored.) In fact, this coexistence of neutral and ionic species was not confirmed by careful optical measurements using polarized light and single crystals.[11,12] In these experiments, all DA pairs undergo the same charge transfer which was estimated to be about 0.5 e^-.

Bond length variations or combinations of them have also been used to estimate ρ in these NIT compounds. Upon ionization, these variations are related to the bonding or antibonding character of the frontier orbital involved on each bond. For isolated D and A molecules, first-principles DFT calculations showed that these variations are indeed linear.[28,29] These linear properties were used in the DMTTF−CA crystal to estimate the charge transfer variation from the HT phase to the LT phase.[8] Assuming a charge transfer of 0.2 e^- in the HT phase and using the variations of inner bond lengths of CA molecules (i.e., C−C and C═C of the phenyl), the coexistence of neutral and ionic species was obtained with neutral species located in planes pl1 and ionic species in planes pl2.

Figures 2 and 3 show bond length variations as a function of ρ. The straight lines correspond to the values deduced from geometry optimizations of isolated charged molecules. The squares correspond to experimental bond lengths taken from ref 8 in the HT phase (300 K) and in each plane of the LT phase taking the estimated ρ value obtained by Aoki and co-workers.[10] The experimental variations of the inner C−C bond lengths of CA is in good agreement with our calculated values. Note that the global shift results from the approximation used for exchange-correlation energy and should be disregarded. For the inner C═C of CA, this agreement is poorer: The experimental bond length variations are too large.

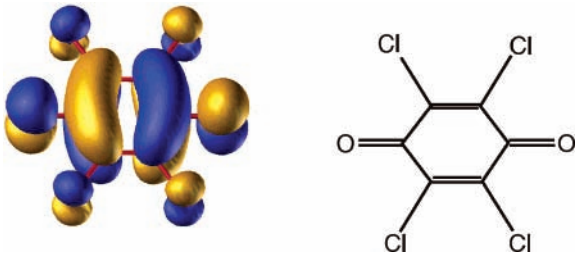

Figure 4. Isosurface plot of the LUMO of CA (right: Lewis representation of CA).

As shown in Figure 3, the variation of C═O bond lengths derived from experiment is consistent with neither the calculated value nor a linear behavior. At 40 K, in the planes pl1 of the LT phase, the C═O bond lengths are longer than those in the planes pl2. In the isolated molecule, the lengths of the bonds increase when charge transfer increases, due to the antibonding character of the LUMO along the C═O bonds (see Figure 4). If this property is transferred to the crystal, the ionicity of the molecules would be larger for those belonging to planes pl1 than those of planes pl2. Using the simple argument consisting of connecting the vibrational frequency of the C═O bond to its length, one finds two different species of molecules: ionic species located in planes pl1 and neutral species located in planes pl2. This is consistent with the findings of Aoki and co-workers[10] but in contradiction to the conclusions given by Collet and co-workers.[8] It is interesting to also consider combinations of C−S and C═C bond length, as proposed by Umland and co-workers[25] and already used to estimate ρ in TTF−CA.[13] Using expression A (B) given in Table 4 of ref 25, one obtains the following estimates for the charge transfer: in the HT phase at 300 K, $\rho = 0.41$ (0.40), and in the LT phase at 40 K, $\rho = 0.57$ (0.57) and $\rho = 0.56$ (0.52) for molecules, respectively, in planes pl1 and pl2. Thus, with this combination of bond lengths, ρ is significantly larger in the HT phase, and below T_c, the ionicities on both layers are almost the same.

This detailed analysis shows that transferring molecular properties such as bond length or variations in vibrational frequencies to crystals is very delicate, so that the resulting estimates of ρ should be taken with caution. From the structural point of view, the existence of different planes is well-established in the LT phase of DMTTF−CA by a fine crystallographic study. It is clear that, once the center of inversion has been lost, the molecules become asymmetric and polarized by intermolecular interactions. This polarization is different for molecules belonging to pl1 and pl2, but it does not necessarily imply that these molecules bear different charges. In this class of molecular crystals, specific intermolecular interactions lead to the nontransferability of the behavior of molecules versus ionicity from gas phase to crystals.

4. Cohesive Energy

The simple model[4] based on the competition between the loss in molecular energy due to the ionization of a DA pair and the Madelung energy gained if the lattice is ionic is very popular in the field of NIT. In this model, the loss in molecular energy is constant and given by IP − EA where IP is the ionization potential of D and EA the electron affinity of A. The gain in Madelung energy is proportional to e^2/a where a is the distance between the centers of mass of D and A along the mixed stacks. For some D−A compounds close to the neutral ionic boundary, it has been observed that the N−I transition can occur due to pressure and temperature.[4,10,30,31] It has been concluded that the

TABLE 1: Madelung (E_{Mad}), Exchange-Correlation (E_{xc}) and Cohesive ($E_{Coh} = E_{Mad} + E_{xc}$) Energies in DMTTF−CA[a]

phase	300 K	40 K	
ρ	0.2	0.3 and 0.6	0.6
E_{Mad}	−0.41	−1.63	−2.58
E_{xc}	−3.90	−3.79	
E_{Coh}	−4.30	−5.42	−6.37

[a] When assuming the following charge transfer in each phase: HT phase at 300 K, 0.2 e^-;[10−12] LT phase at 40 K, (i) 0.3 e^- for pl1 and 0.6 e^- for pl2,[8,10] and (ii) 0.6 e^- for both planes.[11,12]

N−I transition is controlled by the gain in electrostatic Madelung energy due to the contraction of the network (especially *a*) that is induced when decreasing the temperature or increasing the pressure.

4.1. Description of our Simple Model. To estimate the cohesive energy as a function of ρ, we use a simple model based on ab initio calculations for isolated molecules and pair potentials. If the state where the charge transfer vanishes ($\rho = 0$) is used as the reference state, the total energy can be written as

$$E_{tot}(\rho) = E_{mol}(\rho) + E_{Coh}(\rho) \quad (1)$$

The first contribution E_{mol} corresponds to the molecular energy deduced from ab initio calculations on isolated molecules when using the molecular conformation that they adopt in the crystal.[32]

$$E_{mol}(\rho) = \rho(\epsilon_A^0 - \epsilon_D^0) + \frac{1}{2}\rho^2(U_D + U_A) \quad (2)$$

where ϵ_j^0 is the energy of the relevant orbital: HOMO (highest occupied molecular orbital) of D and LUMO (lowest unoccupied molecular orbital) of A, in the reference state ($\rho = 0$). The term U_j corresponds to the Coulomb repulsion of an electron in that orbital. The second contribution in expression 1 corresponds to the cohesive energy between molecules. It is decomposed in two terms

$$E_{Coh}(\rho) = \frac{1}{2}\sum_{i,j}\frac{q_i q_j}{r_{ij}} + \frac{1}{2}\sum_{i,j}\left[B_{ij}\exp(-C_{ij}r_{ij}) - \frac{A_{ij}}{r_{ij}^6}\right] \quad (3)$$

where *i* and *j* denote two atoms each belonging to a different molecule (as E_{mol} already includes all intramolecular contributions to the total energy). The first sum corresponds to the intermolecular Madelung contribution (E_{Mad}) to the electrostatic energy between atomic point charges $\{q_i\}$. The atomic charges q_i's are deduced from PAW calculations on isolated molecules bearing a given charge ρ by using a model density reproducing the multipole moments of the true molecular charge density.[22] The second sum corresponds to the exchange-correlation energy between molecules denoted here by E_{xc} and is usually called van der Waals energy. The empirical parameters A_{ij}, B_{ij}, and C_{ij} are taken from the literature.[33,34] They have been fitted for molecular crystals with atomic point charges.

4.2. Cohesive Energy. Starting from experimental estimations of ρ,[8,10−12] we used this model to estimate each contribution to the cohesive energy in the HT and the LT phases. Our results concerning the values of E_{Mad}, E_{xc}, and E_{Coh} are given in Table 1. In the HT phase, the contribution of E_{xc} is predominant, because it represents 90% of E_{Coh}. When considering the same value for ρ in both planes in the LT phase, which is consistent with the findings of Horiuchi and co-workers,[11,12] the Madelung contribution represents 40% of E_{Coh}. These results are very similar to those obtained for TTF−CA.[16] The Madelung contribution becomes less important, about 30% of E_{Coh}, when considering an alternation of neutral (0.3 e^-) and ionic planes (0.6 e^-) in the LT phase.[8,10] When ρ is fixed and going from the HT structure to the LT one, the corresponding lattice contraction and molecular distortions do not significantly affect the Madelung contribution: for $\rho = 0.2$ e^-, E_{Mad} changes less than one-hundredth of an elctron volt.

TABLE 2: Energies of the Frontier Molecular Orbitals, LUMO of CA (ϵ_A^0) and HOMO of DMTTF (ϵ_D^0); Coulomb Repulsion of an Electron on These Orbitals, Respectively, U_A and U_D; and Ionization Energetic Cost of a DMTTF−CA Pair (IP − EA) for the Molecular Conformations at 300 K (HT Phase) and 40 K (LT Phase) in pl1 and pl2[a]

		40 K		
geometry	300 K	plane pl1	plane pl2	optimized[b] [35,28]
ϵ_A^0	−5.09	−5.21	−5.23	−5.25
ϵ_D^0	−3.73	−3.64	−3.70	−3.90
U_A	5.12	4.99	4.98	4.76
U_D	4.53	4.61	4.59	4.30
IP − EA	3.46	3.23	3.26	3.10

[a] All quantities are expressed in eV. [b] Comparison with the values obtained for the optimized geometry.[35,28]

4.3. Molecular Energy. In comparison with molecules in their optimized geometries (see Table 2), the absolute values obtained for U_i and ϵ_j^0 are slightly larger and weaker, respectively. The cost in energy to ionize a DA pair IP − EA is obtained for $\rho = 1$. In the LT phase, the values of IP − EA for pl1 and pl2 are pretty close but are significantly lower (about 0.2 eV) than the corresponding values in the HT phase.

4.4. Equilibrium Charge Transfer. In our pair potential model, E_{xc} does not depend on ρ (eq 3). Thus, the equilibrium charge transfer ρ_{eq} is given by the minimum of $E_{Mad}(\rho) + E_{mol}(\rho)$. In the HT phase, ρ_{eq} is found to be 0.51 e^- and, in the LT phase, 0.63 and 0.62 e^-, respectively, for pl1 and pl2 (see Table 7).

In comparison with the experimental values of ρ, our model seems to overestimate ρ_{eq} in the HT phase at least by a factor of two. This difference can be explained by the simplicity of our model: The poor description of the intermolecular part of exchange-correlation energy (E_{xc}) is especially sensitive in the neutral phase where it is the dominant term. In fact, this term obviously should depend on the charge transfer between D and A molecules. Moreover, the electrostatic contribution is limited to the first term of its multipolar expansion, and no special treatment of hydrogen bonds is included. Finally, polarization of a given molecule by its neighbors, which would imply a self-consistent treatment, is also missing.

As it concerns the LT phase, our simple model does not lead to an alternation of neutral and ionic planes along the *c* direction, with the charge transfer being almost the same in both types of planes. This result is consistent with the experimental findings of Horiuchi and co-workers[11,12] but also with the estimate deduced in Section 3.2 from a combination of DMTTF's C═C and C−S bond lengths.

According to this molecular model, the degree of ionicity of molecules partly depends on the competition between IP − EA and E_{Mad} contributions to the total energy. However, our calculations do not reveal a significant gain in Madelung energy at constant ρ in the LT phase compared to the HT phase. On the other hand, the decrease of the energy cost of IP − EA

TABLE 3: Potential Energy Density $V(\mathbf{r}_{cp})$ in kJ mol^{-1} of the Strongest Intrachain Contacts for the HT (300 K) and LT (40 K) Phases[a]

		40 K			
		plane pl1		plane pl2	
contact	300 K	intra	inter	intra	inter
C···S	−10.1	−15.8	−8.5	−16.9	−9.4
C···C	−6.1	−10.6		−11.1	
Cl···S (average)	−7.0	−9.6	−7.9	−9.1	−8.2

[a] At 40 K, "intra" and "inter" stand for interaction inside a DA pair and between two DA pairs in pl1 or pl2.

induced by molecular deformations is significant, a result that has always been disregarded in previous theoretical works.[4,10,30,31]

5. Ab Initio Calculations in Crystal

5.1. Valence and Conduction Bands. As for TTF-2,5Cl_2-BQ[23] and TTF−CA,[16] the dispersion of the valence band (VB) and conduction band (CB) in DMTTF−CA is quasi-one-dimensional along the Γ−X direction. Because of a separation by more than 1 eV from the other occupied and unoccupied bands, VB and CB form a nearly two-band system (four bands in the LT phase) which can be described within the framework of a tight binding model, resulting from a combination of the HOMO of D and the LUMO of A. In the HT phase, this hybridization is symmetry-forbidden at Γ because of the inversion symmetry, and the VB is fully located on DMTTF. In the LT phase, the presence of two inequivalent chains in the unit cell induces the VB and CB to be 2-fold. As inversion symmetry is lost, hybridization occurs at Γ, and the gap becomes larger. The tight binding modeling of the HT phase leads to a transfer integral of 0.15 eV, which is slightly lower than the values obtained for TTF−CA[16] and TTF-2,5Cl_2BQ,[23] respectively, 0.17 and 0.18 eV.

5.2. Intermolecular Interactions. From a topological analysis,[16,17,24] we can quantify each electronic intrachain contact using the value of the potential density at the critical point denoted $V(\mathbf{r}_{CP})$. As shown in Table 3, the connection from an S atom of DMTTF to a C atom connected to a Cl atom (Figure 5, red bond paths) of CA corresponds to the strongest contact. It results mainly from the HOMO−LUMO overlap. Other contacts from DMTTF to CA are the ones which imply C···C (green) and S···Cl (blue) bonds. In the LT phase (40 K), the pairing of the molecules in DA pairs induces a strengthening of the contacts inside pairs and a diminution between two pairs. As shown in Table 3, the S···C contact remains the dominant one with a 60% and 70% increase in the planes pl1 and pl2, respectively. The strengthening of the C···C interaction is the most important: respectively, 74% and 82% inside pairs of the planes pl1 and pl2. Not only does the strength of these C···C interactions change at the transition, but also the associated bond-path undergoes bifurcation. In the HT phase, one C atom of the central C═C bond is connected to a C atom of a C−Cl bond, whereas these bond paths jump and connect the other C atom of the C═C central bond to the C atom of a C═O bond of CA molecule (respectively along and across the DMTTF molecule for plane pl1 in Figure 5b and for plane pl2 in Figure 5c). Because of the molecular deformations, the Cl···S contacts are less affected: Their strength increases by 37% and 30% inside pairs of the planes pl1 and pl2, respectively. Figure 5b,c shows strong evidence of the loss of inversion both inside and between the planes. We have not observed relevant differences concerning the nature and strength of the strongest intrachain electronic contacts (heavy red and blue lines) when comparing

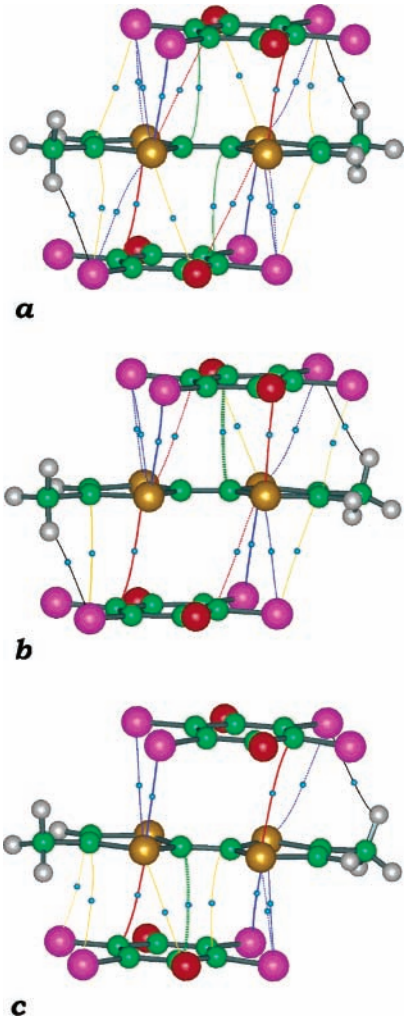

Figure 5. Critical points and bond paths associated to the strongest intrachain contacts in (a) DMTTF−CA at 300 K, (b) plane pl1 of DMTTF−CA at 40 K, and (c) plane pl2 of DMTTF−CA at 40 K. Carbon, sulfur, chlorine, oxygen, and hydrogen atoms are respectively colored in green, gold, purple, red, and gray. Color for bond paths is red for C···S, blue for Cl···S, and green for C···C.

the mixed chains pertaining to the planes pl1 and pl2. Nevertheless, the appearance of the bond path graphs reveals some kind of antiferroelectric behavior. These results are in favor of a small difference concerning the ionicity of molecules. Moreover, the modifications of intra- and intermolecular electronic interactions are similar to those observed in TTF−CA.[16] As ρ essentially results from the HOMO−LUMO overlap along the mixed stacks (i.e., intrachain bonds), ρ should be very comparable in both pairs of the LT phases of DMTTF−CA and TTF−CA. The real changes from pl1 to pl2 in the bond paths concern weaker intrachain contacts.

The strongest interchain bond paths are represented in Figure 6 in the HT phase at 300 K. They can be split in two groups. The first group corresponds to the contacts like O···H (heavy red lines) or S···Cl (heavy and simple blue lines) involving molecules belonging to the same type of planes parallel to (*a*, *b*). The second group involves the interplane contacts O···H_3C (dotted red lines) and Cl···Cl (heavy purple lines) mainly in the *c* direction specific to each D−A crystal.[23] Table 4 shows clearly that the hydrogen bonds dominate all other interchain contacts. The contacts of the first group are very similar to those observed in TTF−CA[13,16] and are located near the O···H bond. In the LT phase, the loss of inversion symmetry leads to two inequivalent distances for each contact (Table 5). The contrac-

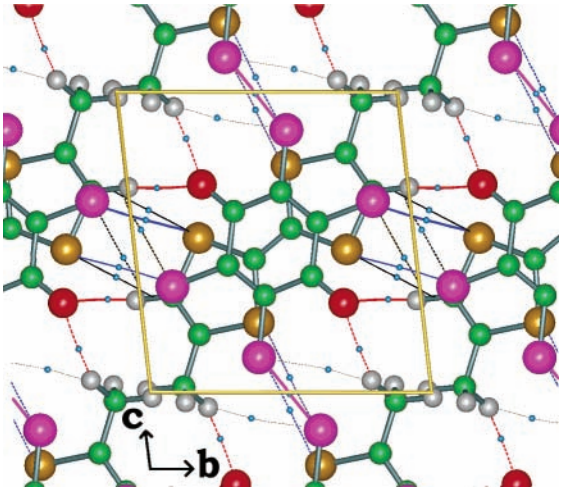

Figure 6. Critical points associated to the strongest interchain contacts in DMTTF−CA at 300 K. Carbon, sulfur, chlorine, oxygen, and hydrogen atoms are respectively colored in green, gold, purple, red, and gray. Color of bond paths is red for O···H, purple for Cl···Cl, and blue for S···Cl.

TABLE 4: Strongest Interchain Contacts for the HT Phase (300 K)

	$V(\mathbf{r}_{cp})^a$	d^b
O···H	−18.5	2.30
S···Cl	−8.5	3.48
O···H_3C^c	−10.4	2.51
Cl···Cl	−11.0	3.43

[a] $V(\mathbf{r}_{cp})$ corresponds to the potential energy density (kJ mol^{-1}) at the critical point. [b] d corresponds to the distance (Å) between the two atoms of the first column. [c] Distance between O and the nearest H of the methyl group.

TABLE 5: Strongest Interchain Contacts along the OH Chains for the LT Phase (40 K) in the Planes pl1 and pl2

		$V(\mathbf{r}_{cp})^a$	Δd^b
	plane pl1		
O···H	short	−26.6	−4.8%
	long	−24.0	−3.5%
S···Cl	short	−10.6	−2.0%
	long	−10.1	−2.3%
	plane pl2		
O···H	short	−31.6	−7.4%
	long	−25.9	−4.8%
S···Cl	short	−11.2	−3.2%
	long	−10.2	−2.0%

[a] $V(\mathbf{r}_{cp})$ corresponds to the potential energy density (kJ mol^{-1}) at the critical point. [b] Δd gives the relative variation of this distance with respect to its value at 300 K.

tion of the unit cell when decreasing the temperature, induces a strengthening of the contacts: Hydrogen bonds are the most affected and become 71% and 40% stronger for the short and long bonds, respectively, in pl2 and 44% and 30%, respectively, in pl1. This strengthening is directly correlated to the reduction of the O···H distances. Other contacts undergo a weaker strengthening, on the order of 15%. Along the *c* direction, the four inequivalent O···H_3C contacts undergo different variations when going from the HT phase to the LT phase (Tables 4 and 5). As expected, these interchain contacts are less sensitive to the charge transfer. No change in the topological graph can be depicted over the entire range of observed bond-paths. Their behavior depends more on the local structural modification. Interestingly, the Cl−Cl interactions are significantly stronger than those observed in TTF−CA. This has to be related to the

TABLE 6: Strongest Interchain Contacts between the Planes pl1 and pl2 for the LT Phase (40 K)

	$V(\mathbf{r}_{cp})^a$	Δd^b
O···H_3C (1)	−16.1	−4.2%
O···H_3C (2)	−12.7	−2.4%
O···H_3C (3)	−11.1	−0.8%
O···H_3C (4)	−8.7	+2.0%
Cl···Cl (1)	−12.7	−1.5%
Cl···Cl (2)	−12.0	−0.9%

[a] $V(\mathbf{r}_{cp})$ corresponds to the potential energy density (kJ mol^{-1}) at the critical point. [b] Δd gives the relative variation of this distance with respect to its value at 300 K.

TABLE 7: Estimates of Charge Transfer ρ from DMTTF to CA

		40 K	
phase	300 K	plane pl1	plane pl2
Bader	0.50	0.63	0.63
molecular model	0.51	0.63	0.62
expt[10,8]	0.2	0.3	0.6
expt[11,12]	0.2	0.5	0.5

different orientations of neighboring CA molecules in the *c* direction, as in TTF−CA where two neighboring CA molecules are deduced from each other by a gliding plane. In TTF-2,5Cl_2-BQ, such Cl−Cl interactions do not occur, because the acceptor has only two Cl atoms. Nevertheless, these Cl−Cl contacts are not largely modified by the NIT, because the values observed for Δd are comparable to the decrease resulting from the lattice contraction. Finally, the structure is almost topologically invariant from the point of view of the strongest bonds: Their strengthening (diminution) defined by $V(\mathbf{r}_{CP})$ is directly correlated to the reduction (increase) in distance according to the relationship obtained for TTF−CA.[16]

5.3. Charge Transfer from Bader's Theory. Within Bader's approach, a basin can be uniquely associated to each atom.[17,24] Atomic moments, in particular, atomic charges, are obtained by integration over the whole basin, and ρ can be estimated by summing the atomic charges belonging to each molecule. The corresponding ρ values are reported in Table 7. Results are very close to those obtained within our simple molecular model despite its simplicity. We confirm using Bader's theory that the ionicity of molecules in the LT phase is almost identical in planes pl1 and pl2, in agreement with the value deduced from the experimental absorption spectra performed on a single crystal.[11,12]

6. Discussion

In this class of D−A crystals, the molecular stacks are very similar: In the framework of a tight binding model, the two-band system constituted by the valence and conduction bands results from a linear combination of the HOMO of D and the LUMO of A. This hybridization induces a transfer of electrons from D to A. In the HT phase, hybridization is forbidden around the center of the Brillouin zone because of the inversion symmetry. The structural phase transition, which is characterized by a symmetry breaking, is accompanied by a significant increase of ρ resulting from hybridization at Γ.

The similarity of D−A crystals is well-confirmed by the topological study of the electron density. In DMTTF−CA, the strongest intrachain molecular interactions are comparable in nature and intensity to those observed in TTF−CA[16] and TTF-2,5Cl_2BQ.[24] They imply the same atoms, and on the basis of the potential energy density at the critical point, their intensities do not differ by more then 10%. In the LT phase, contacts are

reinforced within a given pair, by up to 80%. Contacts between two different pairs can either increase or decrease and are much less affected by the NIT. No appreciable difference concerning the strengthening of contacts has been evidenced between pl1 and pl2, and this strengthening is globally equivalent in both planes.

We showed that interchain contacts can be split in two groups: The first one involves coplanar molecules belonging to a same (*a, b*) plane. Hydrogen bonds are dominant, and their intensity is 50% greater than the strongest intrachain contact. The strengthening of O···H bonds is quite important in the LT phase, from 40% to 70%, and has to be related to the coupling between hydrogen bonds and charge transfer.[35] This first group of contacts also shows up in other D−A crystals. The second group of intermolecular contacts, which corresponds to contacts mainly along the *c* direction, is specific to each crystal. In DMTTF−CA, the most significant contacts correspond to the O···H_3C and Cl−Cl interactions, none of them undergoing a significant reinforcement as compared to the one expected from the lattice contraction.

All these results show that in these D−A crystals HOMO−LUMO overlap and hydrogen bonds dominate the intermolecular interactions in both HT and LT phases and drive the molecular deformation and reorientation which occur at the NIT. All other interchain contacts are dragged along with the former as they do not show any peculiar behavior. In DMTTF−CA, TTF−CA, and, to a lesser extent, TTF-2,5Cl_2BQ, many strong interactions inside and between the chains involve Cl atoms. Interestingly, the Cl−Cl contacts (along the *c* direction) in DMTTF−CA are significantly stronger than those observed in TTF−CA, while they do not occur in TTF-2,5Cl_2BQ. All of the interactions involving Cl must largely contribute to stabilizing these crystal structures.

Our estimation of charge transfer ρ using a simple molecular model based on ab initio calculations in isolated molecules and pair potentials leads to an overestimation of the value of ρ in the HT phase. The integration of electron density over atomic basins gives the same result. This systematic overestimation results from the poor description of the van der Waals dynamical interactions. In the LT phase, the effect is less dramatic, because electrostatic interactions become dominant. Our different results show no difference between the values of ρ in planes pl1 and pl2, in agreement with the estimates deduced from polarized IR reflection measurements on single crystals.[11,12] Thus, we believe that there is no coexistence of neutral and ionic species at low temperature, and therefore, no periodic ordering of N and I layers in DMTTF−CA. The existence of two structurally different planes perpendicular to the *c* direction is not in question. However, it does not necessarily imply that molecules in pl1 and pl2 bear different charges. These molecules are far from being point charges; they become asymmetric and can easily polarize because of different intermolecular interactions.

Finally, our results show that the simple model based on the competition between the cost of ionizing a DA pair IP − EA and the Madelung energy gained if the lattice is ionic should be used with great care. It appears that IP − EA is significantly modified by the changes in the molecular geometries, which are, when going from the HT to the LT phase, about 0.2 eV for a DA pair pertaining to either pl1 or pl2. On the other hand, the gain in Madelung energy due to the contraction of the unit cell at constant ρ is much smaller and thus should not be considered as the key parameter for crossing the neutral ionic boundary and thus for the NIT.

Acknowledgment. The authors would like to thank C. Koenig for useful discussion and are grateful to P.E. Blöchl for his PAW code. Calculations have been supported by the "Centre Informatique National de l'Enseignement Supérieur" (CINES−France). This work has benefited from collaborations within (1) the Ψ_k-ESF Research Program, (2) the Training and Mobility of Researchers Program "Electronic Structure" (Contract: FMRX-CT98-0178) of the European Union, and (3) the International Joint Research Grant "Development of charge transfer materials with nanostructures" (Contract: 00MB4).

References and Notes

(1) Collet, E.; Cailleau, M.-H. L.; Le Cointe, M. B.; Cailleau, H.; Wulff, M.; Luty, T.; Koshihara, S.-Y.; Meyer, M.; Toupet, L.; Rabiller, P.; Techert, S. *Science* **2003**, *300*, 612.

(2) Collet, E.; Cailleau, M.-H. L.; Le Cointe, M. B.; Cailleau, H.; Ravy, S.; Luty, T.; Bérar, J.-P.; Czarnecki, P.; Karl, N. *Europhys. Lett.* **2002**, *57*, 67.

(3) Mayerle, J. J.; Torrance, J. B.; Crowley, J. I. *Acta Crystallogr., Sect. B* **1979**, *35*, 2988.

(4) Torrance, J. B.; Vazquez, J. E.; Mayerle, J. J.; Lee, V. Y. *Phys. Rev. Lett.* **1981**, *46*, 253.

(5) Koshihara, S. Y.; Takahashi, Y.; Sakai, H.; Tokura, Y.; Luty, T. *J. Phys. Chem. B* **1999**, *103*, 2592.

(6) Girlando, A.; Marzolai, F.; Pecile, C.; Torrance, J. B. *J. Chem. Phys.* **1983**, *79*, 1075.

(7) Jacobsen, C. S.; Torrance, J. B.; Crowley, J. I. *J. Chem. Phys.* **1983**, *78*, 112.

(8) Collet, E.; Le Cointe, M. B.; Cailleau, M.-H. L.; Cailleau, H.; Toupet, L.; Meven, M.; Mattauch, S.; Heger, G.; Karl, N. *Phys. Rev. B* **2001**, *63*, 054105.

(9) Nogami, Y.; Taoda, M.; Oshima, K.; Aoki, S.; Miura, A. *Synth. Met.* **1995**, *70*, 1219.

(10) Aoki, S.; Nakayama, T.; Miura, A. *Phys. Rev. B* **1993**, *48*, 626.

(11) Horiochi, S.; Okimoto, Y.; Kumai, R.; Tokura, Y. *J. Am. Chem. Soc.* **2001**, *123*, 665.

(12) Horiochi, S.; Kumai, R.; Okimoto, Y.; Tokura, Y. *Synth. Met.* **2003**, *133−134*, 615.

(13) Le Cointe, M. B.; Cailleau, M.-H. L.; Calleau, H.; Toupic, B.; Toupet, L.; Heger, G.; Moussa, F.; Schweiss, P.; Kraft, K. H.; Karl, N. *Phys. Rev. B* **1995**, *51*, 3374.

(14) Hubbard, J.; Torrance, J. B. *Phys. Rev. Lett.* **1981**, *47*, 1750.

(15) Iwai, S.; Tanaka, S.; Fujinuma, K.; Kishida, H.; Okamoto, H.; Tokura, Y. *Phys. Rev. Lett.* **2002**, *88*, 057402.

(16) Oison, V.; Katan, C.; Rabiller, P.; Souhassou, M.; Koenig, C. *Phys. Rev. B* **2003**, *67*, 035120.

(17) Bader, R. F. W. *Atoms in Molecules: A quantum theory*; The International Series of Monographs on Chemistry; Clarendon Press: Oxford, 1990.

(18) Perdew, J. P.; Zunger, A. *Phys. Rev. B* **1981**, *23*, 5048.

(19) Becke, A. D. *J. Chem. Phys.* **1992**, *96*, 2155.

(20) Perdew, J. P. *Phys. Rev. B* **1986**, *33*, 8822.

(21) Blöchl, P. E. *Phys. Rev. B* **1994**, *50*, 17953.

(22) Blöchl, P. E. *J. Chem. Phys.* **1995**, *103*, 7422.

(23) Katan, C.; Koenig, C. *J. Phys.: Condens. Matter* **1999**, *11*, 4163.

(24) Katan, C.; Rabiller, P.; Lecomte, C.; Guezo, M.; Oison, V.; Souhassou, M. *J. Appl. Crystallogr.* **2003**, *36*, 65.

(25) Umland, T. C.; Allie, S.; Kuhlmann, T.; Coppens, P. *J. Phys. Chem.* **1988**, *92*, 6456.

(26) Girlando, A.; Bozio, R.; Pecile, C.; Torrance, J. N. *Phys. Rev. B* **1982**, *26*, 2306.

(27) Hanfland, M.; Brillante, A.; Girlando, A.; Syassen, K. *Phys. Rev. B* **1998**, *38*, 1456.

(28) Katan, C.; Blöchl, P. E.; Margl, P.; Koenig, C. *Phys. Rev. B* **1996**, *53*, 12112.

(29) Katan, C. *J. Phys. Chem. A* **1999**, *103*, 1407.

(30) Torrance, J. B.; Girlando, A.; Mayerle, J. J.; Crowley, J. I.; Lee, V. Y.; Batail, P. *Phys. Rev. Lett.* **1981**, *47*, 1747.

(31) Brillante, A.; Girlando, A. *Phys. Rev. B* **1992**, *45*, 7026.

(32) Carloni, P.; Blöchl, P. E.; Parrinello, M. *J. Phys. Chem.* **1995**, *99*, 1338.

(33) Houpt, D.; Williams, D. E. *Acta Crystallogr., Sect. A* **1986**, *42*, 286.

(34) Hsu, H. Y.; Williams, D. E. *Acta Crystallogr., Sect. A* **1980**, *36*, 277.

(35) Oison, V.; Katan, C.; Koenig, C. *J. Phys. Chem. A* **2001**, *17*, 4300.